International Journal of Mass Spectrometry 303 (2011) 137–146

Contents lists available at ScienceDirect

International Journal of Mass Spectrometry

journal homepage: www.elsevier.com/locate/ijms

Determination of absolute photoionization cross-sections of nitrogenous compounds

Mingfeng Xie, Zhongyue Zhou, Zhandong Wang, Dongna Chen, Fei Qi*

National Synchrotron Radiation Laboratory, University of Science and Technology of China, Hefei, Anhui 230029, PR China

ARTICLE INFO

Article history:
Received 12 December 2010
Received in revised form 18 January 2011
Accepted 18 January 2011
Available online 3 February 2011

Keywords:
Absolute photoionization cross-sections
Nitrogenous compounds
VUV photoionization
Mass spectrometry

ABSTRACT

The absolute photoionization cross-sections of 24 nitrogenous compounds were measured in the photon energy range from their respective ionization thresholds to 11.5 eV, including *n*-propylamine, *iso*-propylamine, *n*-butylamine, 2-butylamine, *iso*-butylamine, *tert*-butylamine, diethylamine, dibutylamine, triethylamine, aniline, benzylamine, *n*-methylaniline, cyclohexanamine, nitromethane, nitroethane, nitropropane, nitrobenzene, pyrrole, pyridine, pyrrolidine, morpholine, *N*,*N*-dimethylethanolamine, benzonitrile and benzeneacetonitrile. The experiments were performed by photoionization mass spectrometry with tunable synchrotron vacuum ultraviolet (VUV) light as an ionization source. Binary-liquid-mixtures of investigated and standard species were used in this measurement. As a good solvent, benzene was chosen as a calibration standard, since its photoionization cross-section had been well know. Moreover, photodissociative fragments were also presented.

1. Introduction

One of the important categories of nitrogenous compounds is organically bound nitrogen, which can be found in coal, heavy oils and almost all solid fuels from biomass to waste [1–3]. Combustion of these fuels is a significant source of NOx emission, which can lead to the formation of photochemical smog, ground level ozone, acid rain and consequently has detrimental effects on the environment and human healthy. Many studies have been carried out to investigate the combustion of compounds containing nitrogen, such as nitromethane, pyrrole, pyridine and morpholine with photoionization mass spectrometry (PIMS) method [4–7]. To get a comprehensive understanding of the flame structure and mechanism, quantification of combustion species is of great importance [8]. But this quantification analysis is inaccessible when the photoionization cross-sections of combustion intermediates are unknown.

Unfortunately, there has been only a few works reporting the measurement of cross-sections for some small nitrogenous compounds. Adam and Zimmermann determined the single photon ionization cross-sections of NO at 10.5 eV [9]. Shaw and Holland measured the cross-sections of NO from its ionization threshold to 21 eV with a double ion chamber and the monochromated synchrotron radiation [10]. Masuoka and Kobayashi determined the single and double photoionization cross-sections of NO_2 and the ionic fragmentation of NO_2^+ and NO_2^{2+} in the photon energy region of 37–125 eV by use of the time-of-flight (TOF) mass spectrometer (MS) and the photoion–photoion coincidence method together with synchrotron radiation [11]. Xia et al. measured the photoabsorption and photoionization cross-sections of NH_3 from its ionization threshold to 1060 Å using synchrotron radiation [12]. Suto and Lee [13] measured the cross-sections and quantum yields of emissions from the photofragments of NH_3 in the 106–200 nm region with synchrotron radiation as well. Calculations of cross-sections for some small gas phase nitrogen compounds, like NH_3, were reported by several groups and their results were in good agreement with experimental data [14–16].

In this paper, we presented absolute photoionization cross-sections for 24 nitrogenous compounds in the photon energy range from respective IEs to 11.5 eV, including *n*-propylamine, *iso*-propylamine, *n*-butylamine, 2-butylamine, *iso*-butylamine, *tert*-butylamine, diethylamine, dibutylamine, triethylamine, aniline, benzylamine, *n*-methylaniline, cyclohexanamine, nitromethane, nitroethane, nitropropane, nitrobenzene, pyrrole, pyridine, pyrrolidine, morpholine, *N*,*N*-dimethylethanolamine, benzonitrile and benzeneacetonitrile. The binary-liquid-mixture method was combined with the VUV PIMS. Photodissociative fragments were also presented in this work.

2. Experimental

2.1. Instrumentation

The experiments were carried out at National Synchrotron Radiation Laboratory (NSRL) in Hefei, China. The beamline and

* Corresponding author. Tel.: +86 551 3602125; fax: +86 551 5141078.
E-mail address: fqi@ustc.edu.cn (F. Qi).

1387-3806/$ – see front matter © 2011 Elsevier B.V. All rights reserved.
doi:10.1016/j.ijms.2011.01.024

the experimental apparatus were reported in our previous reports [17–19]. In brief, synchrotron radiation from a bending magnet beamline was dispersed by a 1 m home-made Seya-Namioka monochromator equipped with a grating coated with Au (1200 grooves/mm). The energy resolution ($E/\Delta E$) is about 500. A LiF filter with 0.5 mm thickness was used to eliminate high-order harmonic radiation at photon energies below 11.7 eV.

The experimental setup consists of a source chamber with a gas feeding system, a differentially pumped chamber and a photoionization chamber with a home-made reflection time-of-flight (RTOF) mass spectrometer. The sampled species formed a molecular beam through a quartz nozzle with a 0.3 mm diameter orifice and a nickel skimmer with a 1.25 mm diameter aperture, and passed into the photoionization chamber, where the molecular beam was intersected and ionized by the tunable VUV light. Photoions were propelled into the flight tube by a pulse extraction field triggered by a pulse generator (DG 535, Stanford Research Systems, Inc. Sunnyvale, CA, USA), and then ions were reflected to a microchannel plate (MCP) detector. After amplified by a VT120C preamplifier (EG & G, ORTEC, Oak Ridge, TN, USA), the ion signal was recorded by a P7888 multiscaler (FAST Comtec, Oberhaching, Germany). A silicon photodiode SXUV-100 (International Radiation Detectors Inc., CA, USA) was employed to monitor the photon flux for normalizing the ion signals considering the quantum efficiency of the photodiode.

2.2. Measurement procedure

Binary-liquid-mixture method was applied in this study. The absolute photoionization cross-sections of benzene measured by Rennie et al. [20] were used as the calibration standard in our measurement [17–19]. When the mole ratio of target to standard molecules in the binary mixture equals one, the ratio of target to standard ion signal can be expressed by the equation:

$$\frac{S_T}{S_S} = \left[\frac{\sigma_T(E)}{\sigma_S(E)}\right]\left[\frac{R_T}{R_S}\right] \quad (1)$$

Here the subscript T and S denote the target and standard molecules. $\sigma(E)$ is the photoionization cross-section at the photon energy of E; R is a mass-dependent response factor that accounts for different sampling and detection efficiencies, which has been reported in our previous work [17]. S is the integrated intensity of ion signal, which has been normalized by the photon flux and plotted as a function of the photon energy, yielding the photoionization efficiency (PIE) spectra. Over the energy range from 9.24 eV (the IE of benzene) to 11.5 eV, the absolute photoionization cross-sections of target molecules were obtained by Eq. (1). For species with IEs lower than 9.24 eV, the absolute photoionization cross-sections were obtained by extrapolating their PIE curves to the ionization thresholds. The interference of isotope was also excluded from corresponding ions in the calculation process discussed above.

The binary mixture of benzene and target species at the mole ratio of 1:1 was pumped into the vaporizer with the flow controlled by a high performance liquid chromatograph pump (Fuli Analytical Instrument Co., Ltd., Zhejiang, China). The vaporized mixture was then diluted by argon, the flow rate of which was kept at 0.25 SLM (standard liters per minute) by a MKS mass flow controller. Subsequently, the gas consisting of 5% vaporized mixture and 95% argon was fed into the source chamber through a stainless steel tube, which was heated to avoid being condensing. The distance between the exit of the stainless steel tube and the sampling quartz nozzle was 10 mm. The pressure of the source chamber was kept at 5 Torr, controlled by a MKS throttle valve (MKS Instruments, Andover, MA, USA). No cluster was observed in the experiments.

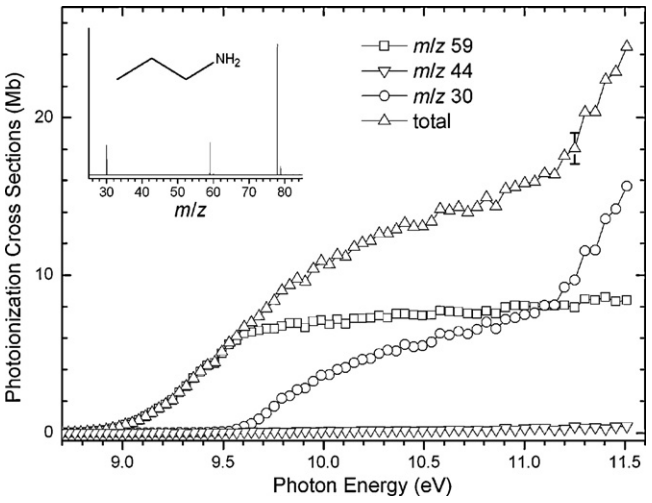

Fig. 1. Absolute photoionization cross-sections of *n*-propylamine. The error bars denote standard deviations of three replicates with separately prepared binary mixtures. The inserted figure displays the photoionization mass spectrum at the photon energy of 10.5 eV.

Iso-Butylamine (≧98%, Fluka) was purchased from Sigma–Aldrich Inc. 2-Butylamine (98%), nitropropane (98%) and pyrrolidine (≧99%) were purchased from Alfa Aesar Inc. *N*,*N*-Dimethylethanolamine (GR) was purchased from Aladdin Reagent Database, Inc. (Shanghai, China). Triethylamine (AR), pyridine (AR) and the others (CP) were all purchased from Sinopharm Chemical Reagent Co., Ltd. (Shanghai, China). All chemicals were used without further purification.

3. Results

Figs. 1–24 show the measured photoionization cross-sections of 24 nitrogenous compounds in this work. The inserted plots in the figures are partial photoionization mass spectra measured at the photon energy of 10.5 eV except for nitromethane, nitroethane and nitropropane at 11.5 eV. The error bars in the figures are standard deviations of 2–4 independent measurements with separately prepared binary mixtures. For most compounds, a reasonable uncertainty of about ±25% is assigned to the exper-

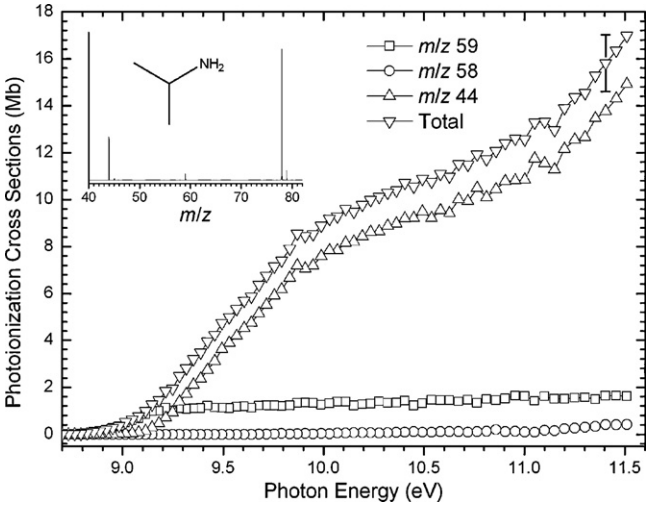

Fig. 2. Absolute photoionization cross-sections of *iso*-propylamine. The error bars denote standard deviations of two replicates with separately prepared binary mixtures. The inserted figure displays the photoionization mass spectrum at the photon energy of 10.5 eV.

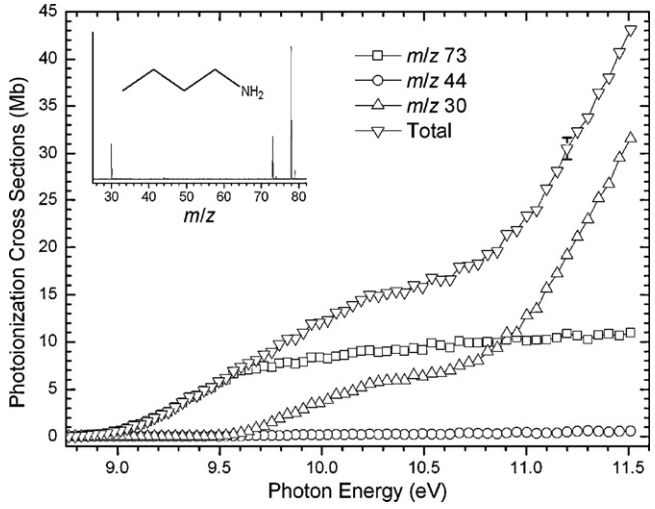

Fig. 3. Absolute photoionization cross-sections of *n*-butylamine. The error bars denote standard deviations of two replicates with separately prepared binary mixtures. The inserted figure displays the photoionization mass spectrum at the photon energy of 10.5 eV.

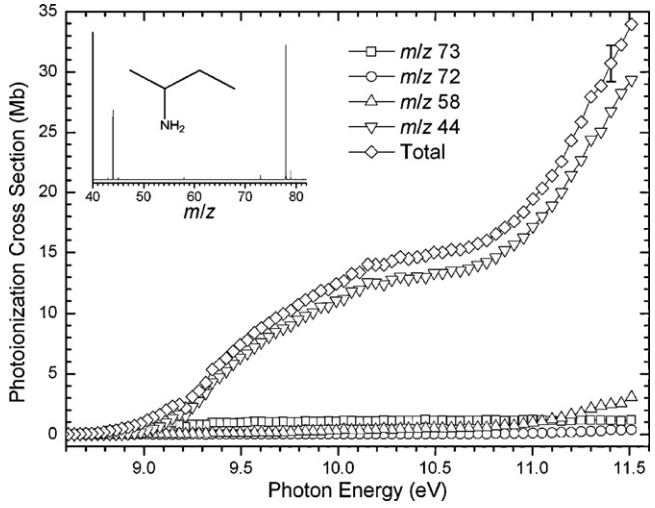

Fig. 4. Absolute photoionization cross-sections of 2-butylamine. The error bars denote standard deviations of three replicates with separately prepared binary mixtures. The inserted figure displays the photoionization mass spectrum at the photon energy of 10.5 eV.

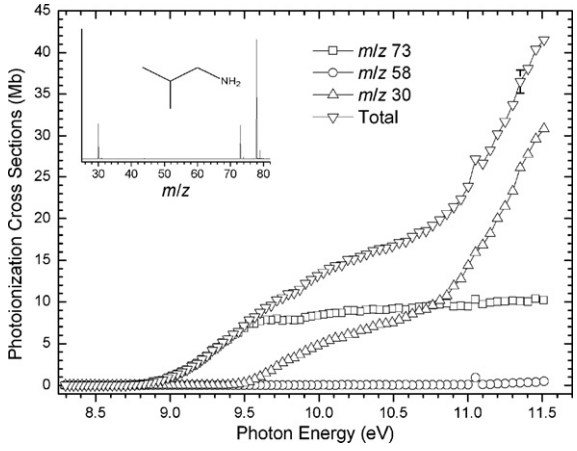

Fig. 5. Absolute photoionization cross-sections of *iso*-butylamine. The error bars denote standard deviations of two replicates with separately prepared binary mixtures. The inserted figure displays the photoionization mass spectrum at the photon energy of 10.5 eV.

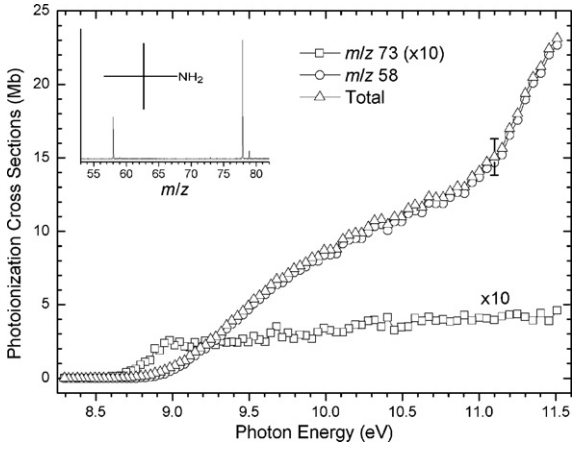

Fig. 6. Absolute photoionization cross-sections of *tert*-butanol. The error bars denote standard deviations of two replicates with separately prepared binary mixtures. The inserted figure displays the photoionization mass spectrum at the photon energy of 10.5 eV.

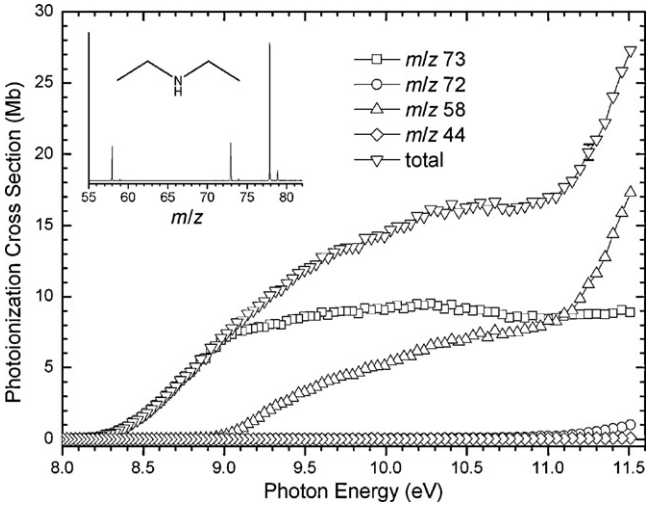

Fig. 7. Absolute photoionization cross-sections of diethylamine. The error bars denote standard deviations of two replicates with separately prepared binary mixtures. The inserted figure displays the photoionization mass spectrum at the photon energy of 10.5 eV.

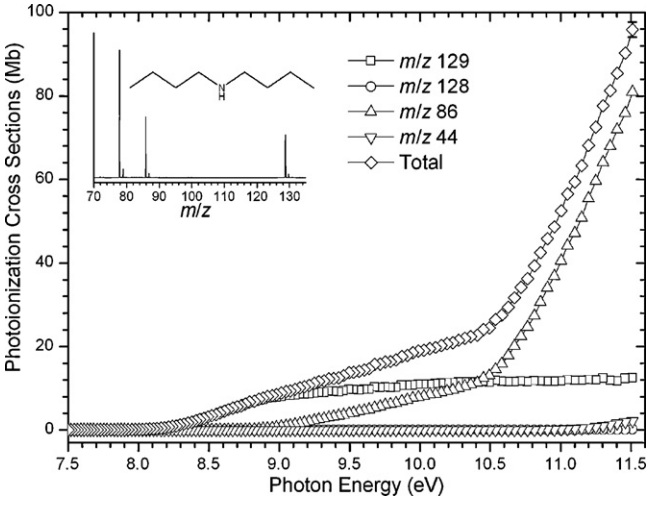

Fig. 8. Absolute photoionization cross-sections of dibutylamine. The error bars denote standard deviations of two replicates with separately prepared binary mixtures. The inserted figure displays the photoionization mass spectrum at the photon energy of 10.5 eV.

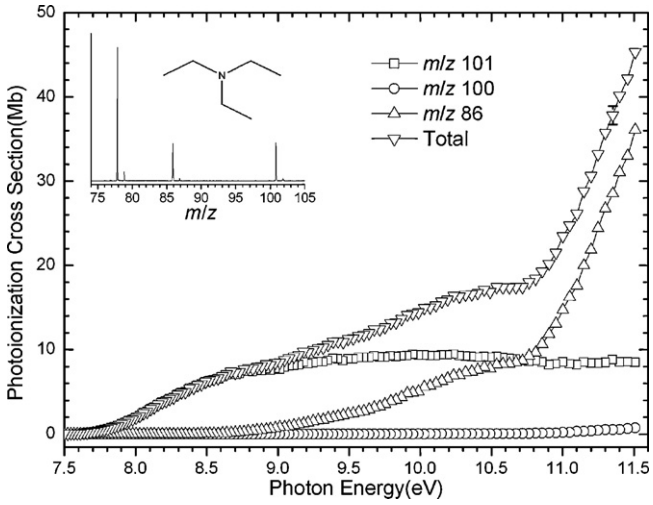

Fig. 9. Absolute photoionization cross-sections of triethylamine. The error bars denote standard deviations of two replicates with separately prepared binary mixtures. The inserted figure displays the photoionization mass spectrum at the photon energy of 10.5 eV.

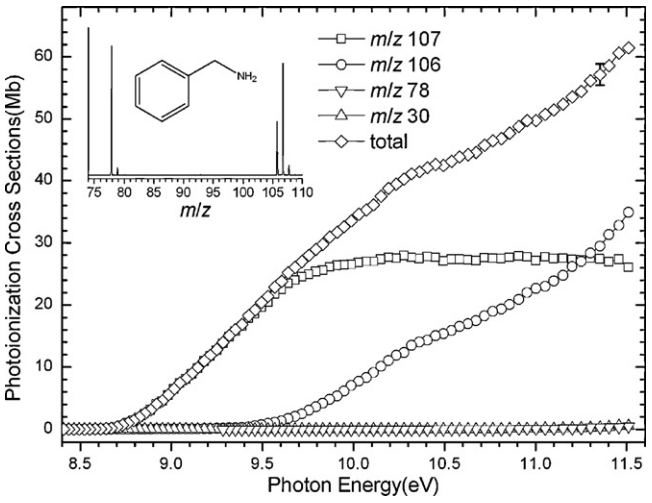

Fig. 11. Absolute photoionization cross-sections of benzylamine. The error bars denote standard deviations of three replicates with separately prepared binary mixtures. The inserted figure displays the photoionization mass spectrum at the photon energy of 10.5 eV.

imental data considering the reproducibility of cross-sections by ±5%, the purity of chemicals, the uncertainty of the cross-section of benzene by ±15%, and the errors of mass discrimination factors by ± 15%. The tabulated data are provided as *supplementary material* of this paper. The detailed description on the investigated molecules is provided below. Ionization energies (IEs) of 24 investigated molecules were extensively measured previously, but the data of their absolute photoionization cross-sections are not available yet.

3.1. *n*-Propylamine and *iso*-propylamine

Figs. 1 and 2 display the absolute photoionization cross-sections of *n*-propylamine and *iso*-propylamine in the photon energy range from their respective IEs to 11.5 eV. As shown in Fig. 1, the photoionization cross-sections of *n*-propylamine (*m*/*z* 59) rise slowly from its ionization threshold to a plateau of 6–8 Mb (10^{-18} cm^2) near 9.60 eV. IE of *n*-propylamine is 8.76 eV, which is in good agreement with the value (8.78 ± 0.02 eV) measured by Watanabe et al. [21]. The main photodissociative fragment from *n*-propylamine is $CH_2NH_2^+$ (*m*/*z* 30) by αC–βC bond cleavage. Its appearance energy (AE) is 9.55 ± 0.05 eV, which accords with literature value (9.54 eV) reported by Chupka [22]. The fragment $CH_2CH_2NH_2^+$ (*m*/*z* 44) producing by demethylation reaction of *n*-propylamine is also observed in this work, but makes little contribution to the total cross-sections.

Iso-Propylamine is an important fine chemical intermediate in organic synthesis of coating materials, plastics, pesticides, rubber chemicals, pharmaceuticals and others [23–25]. In Fig. 2, the cross-section curve of *iso*-propylamine shows the similar trend as *n*-propylamine. IE (8.73 ± 0.05 eV) measured in this work agrees well with the reference value (8.72 ± 0.03 eV) reported by Watanabe et al. [21]. Two photodissociative fragments $CH_3CHNH_2^+$ (*m*/*z* 44) and $CH_3(CH_3)CNH_2^+$ (*m*/*z* 58) were observed in this work. The $CH_3CHNH_2^+$ ion is a major fragment via demethylation reaction, with the AE of 8.95 ± 0.05 eV, which is 0.09 eV higher than the data reported by Solka and Russell [26] and 0.17 eV lower than the value measured by Lossing et al. [27]. The other fragment

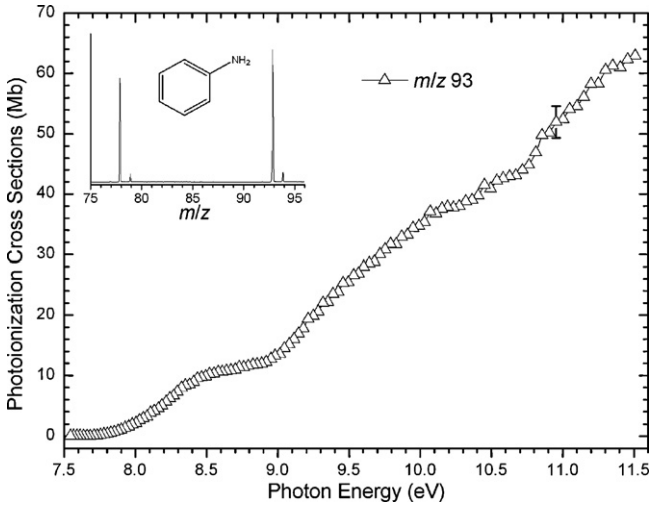

Fig. 10. Absolute photoionization cross-sections of aniline. The error bars denote standard deviations of two replicates with separately prepared binary mixtures. The inserted figure displays the photoionization mass spectrum at the photon energy of 10.5 eV.

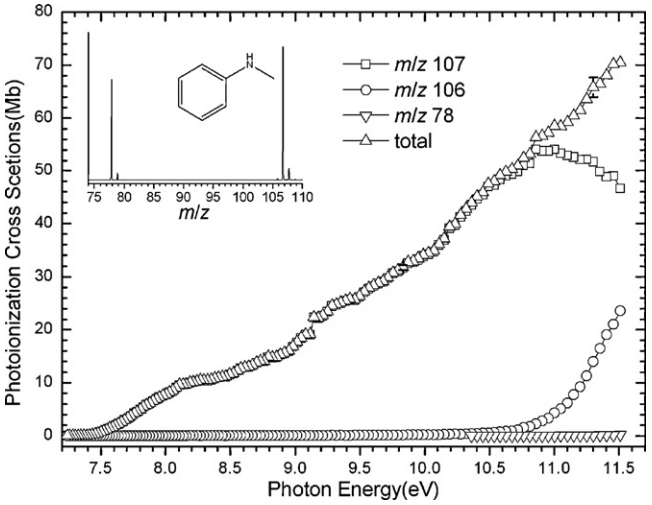

Fig. 12. Absolute photoionization cross-sections of *n*-methylaniline. The error bars denote standard deviations of two replicates with separately prepared binary mixtures. The inserted figure displays the photoionization mass spectrum at the photon energy of 10.5 eV.

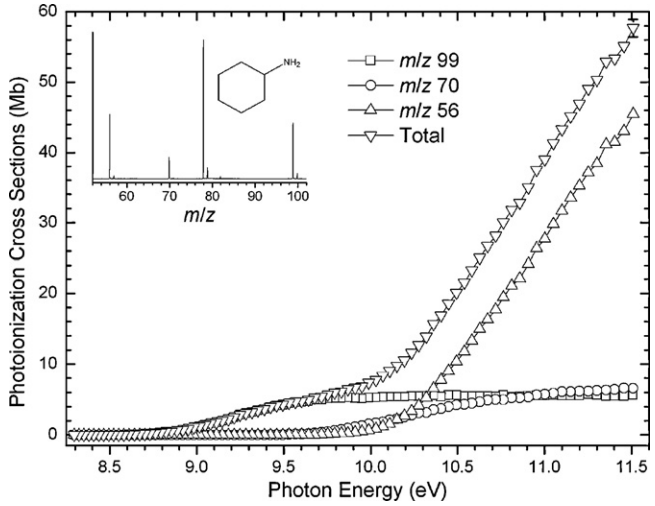

Fig. 13. Absolute photoionization cross-sections of cyclohexanamine. The error bars denote standard deviations of two replicates with separately prepared binary mixtures. The inserted figure displays the photoionization mass spectrum at the photon energy of 10.5 eV.

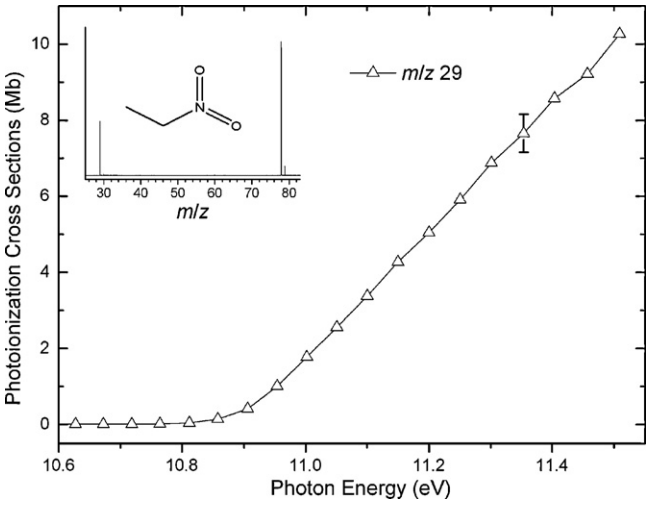

Fig. 15. Absolute photoionization cross-sections of nitroethane. The error bars denote standard deviations of two replicates with separately prepared binary mixtures. The inserted figure displays the photoionization mass spectrum at the photon energy of 11.5 eV.

$CH_3C(CH_3)NH_2^+$ via dehydrogenation of αC makes minor contribution to the total cross-section with the AE of 9.64 ± 0.1 eV, which is much higher than the value (9.2 eV) measured by Lossing et al. [27]. The uncertainty of photoionization cross-section measurement for *n*-propylamine and *iso*-propylamine is less than ±25%.

3.2. *n*-Butylamine, 2-butylamine, iso-butylamine and tert-butylamine

These four isomeric butylamines all can be used as ingredients in the manufacture of pesticides, pharmaceuticals and emulsifiers [28–31]. The absolute photoionization cross-sections of four butylamines are displayed in Figs. 3–6. For *n*-butylamine (Fig. 3), the cross-sections of parent molecule rise slowly up to a plateau of 7–12 Mb from its IE (8.73 ± 0.05 eV), which is in good agreement with the value (8.71 ± 0.03 eV) measured by Watanabe et al. [21]. The major fragment is $CH_2NH_2^+$ (*m*/*z* 30) formed by αC–βC bond cleavage, with the AE of 9.47 ± 0.05 eV, which is lower than the value (9.62 eV) by the electron impact (EI) method [32]. The minor fragment $CH_2CH_2NH_2^+$ (*m*/*z* 44) is formed via βC–γC bond cleavage reaction of *n*-butylamine. And it is observed in this work with AE of 9.18 ± 0.1 eV, which is also lower than the value 9.49 ± 0.09 eV by EI method [26].

Fig. 4 shows the photoionization and photodissociation cross-sections of 2-butylamine. The cross-sections of parent molecule rise up to a plateau from its IE (8.60 ± 0.1 eV), which is 0.1 eV higher than the value by the photoelectron spectroscopy (PE) method [33] and 0.1 eV lower than the value (8.70 eV) measured by Watanabe et al. [21]. The fragment $CH_3CHNH_2^+$ (*m*/*z* 44) coming from the ethyl radical elimination reaction makes major contribution to the total cross-sections from the AE (8.85 ± 0.05 eV), which is 0.06 eV lower than the value (9.10 eV) by EI method [32]. The fragment $CH_3CH_2CHNH_2^+$ (*m*/*z* 58) via elimination of the branch chain methyl radical is minor, with AE of 8.89 ± 0.1 eV, which is lower than the value (9.12 eV) by EI method [27]. The minor fragment $CH_3CH_2C(CH_3)NH_2^+$ (*m*/*z* 72) via dehydrogenation of α-C is also observed in this work.

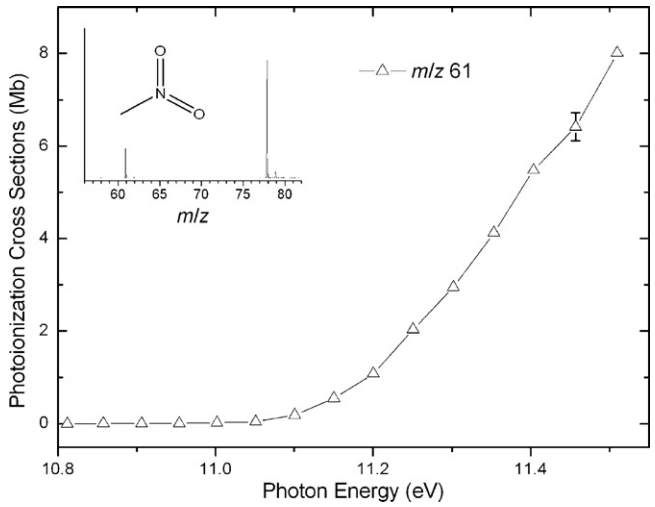

Fig. 14. Absolute photoionization cross-sections of nitromethane. The error bars denote standard deviations of two replicates with separately prepared binary mixtures. The inserted figure displays the photoionization mass spectrum at the photon energy of 11.5 eV.

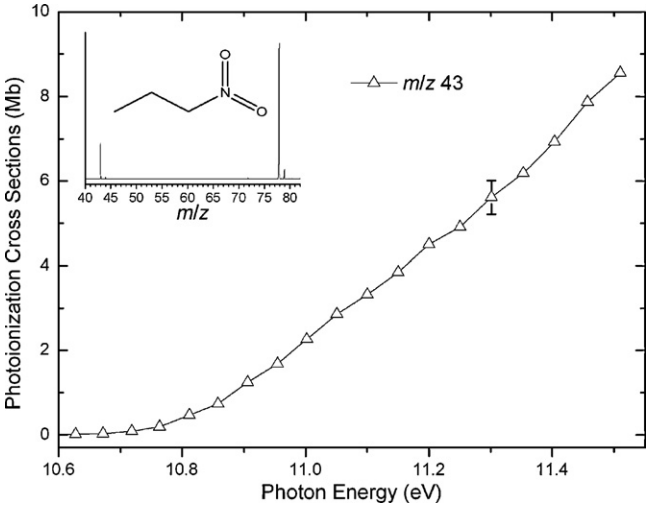

Fig. 16. Absolute photoionization cross-sections of nitropropane. The error bars denote standard deviations of two replicates with separately prepared binary mixtures. The inserted figure displays the photoionization mass spectrum at the photon energy of 11.5 eV.

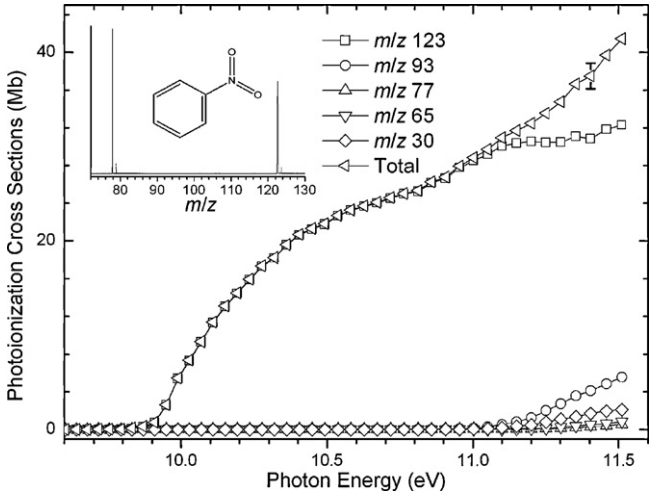

Fig. 17. Absolute photoionization cross-sections of *n*-nitrobenzene. The error bars denote standard deviations of two replicates with separately prepared binary mixtures. The inserted figure displays the photoionization mass spectrum at the photon energy of 10.5 eV.

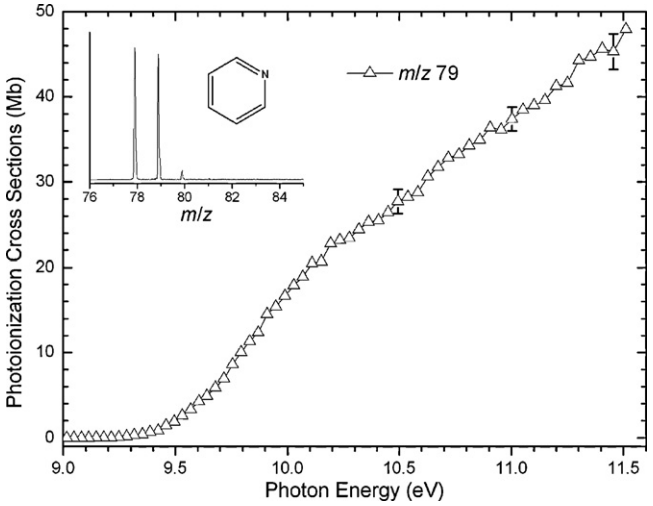

Fig. 19. Absolute photoionization cross-sections of pyridine. The error bars denote standard deviations of two replicates with separately prepared binary mixtures. The inserted figure displays the photoionization mass spectrum at the photon energy of 10.5 eV.

As shown in Fig. 5, the cross-section curve of *iso*-butylamine increases to a plateau from its IE (8.70 ± 0.05 eV), which is in good agreement with the literature value (8.70 eV) measured by Watanabe et al. [21]. The major fragment is $CH_2NH_2^+$ (*m*/*z* 30) by αC–βC bond cleavage, the AE of which is 9.35 ± 0.05 eV, lower than the value (9.52 eV) by EI method [32]. The fragment $CH_3CHCH_2NH_2^+$ (*m*/*z* 58) via demethylation is also observed in this work, but makes minor contribution to the total cross-sections.

For *tert*-butylamine (Fig. 6), the total cross-sections are almost attributed to the major fragment $CH_3C(CH_3)NH_2^+$ (*m*/*z* 58) via demethylation with AE at 8.58 ± 0.05 eV, much lower than the value (8.89 eV) by EI method [27]. IE (8.58 ± 0.1 eV) of $C_4H_{11}N$ agrees well with the literature value (8.64 eV) measured by Watanabe et al. [21] within the permissible error range. The uncertainty for photoionization cross-section measurement of *n*-butylamine, 2-butylamine, *iso*-butylamine and *tert*-butylamine is less than ±25%.

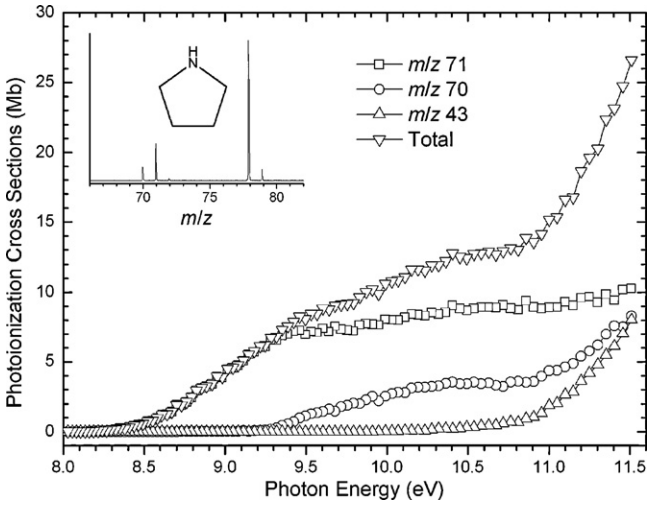

Fig. 20. Absolute photoionization cross-sections of pyrrolidine. The inserted figure displays the photoionization mass spectrum at the photon energy of 10.5 eV.

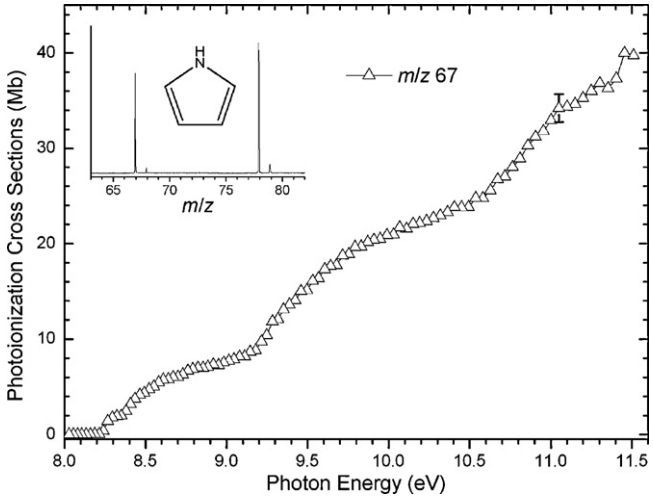

Fig. 18. Absolute photoionization cross-sections of pyrrole. The error bars denote standard deviations of two replicates with separately prepared binary mixtures. The inserted figure displays the photoionization mass spectrum at the photon energy of 10.5 eV.

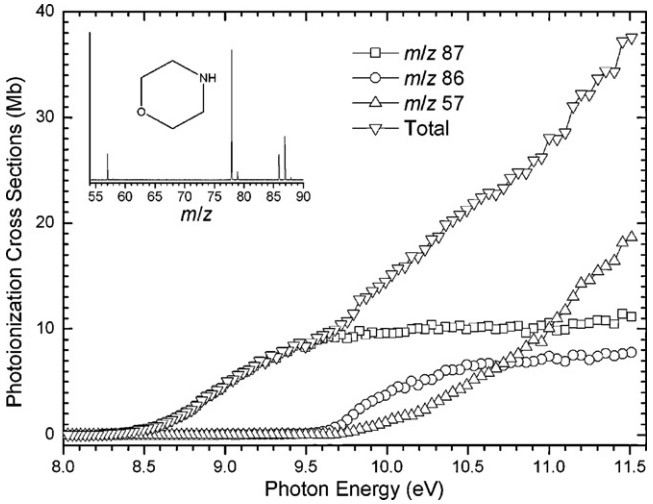

Fig. 21. Absolute photoionization cross-sections of morpholine. The inserted figure displays the photoionization mass spectrum at the photon energy of 10.5 eV.

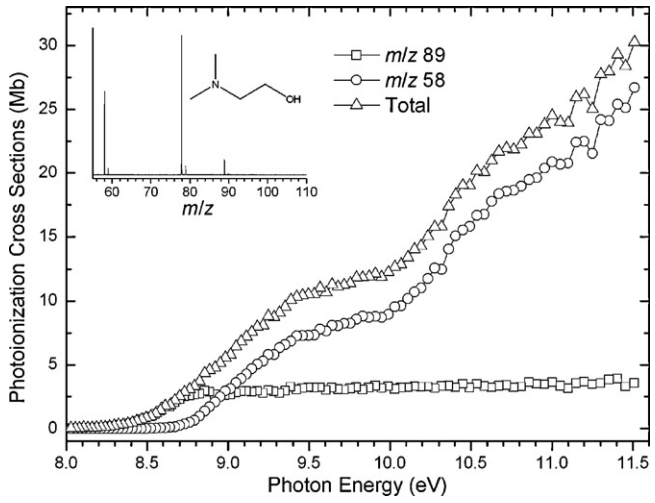

Fig. 22. Absolute photoionization cross-sections of *N*,*N*-dimethylethanolamine. The inserted figure displays the photoionization mass spectrum at the photon energy of 10.5 eV.

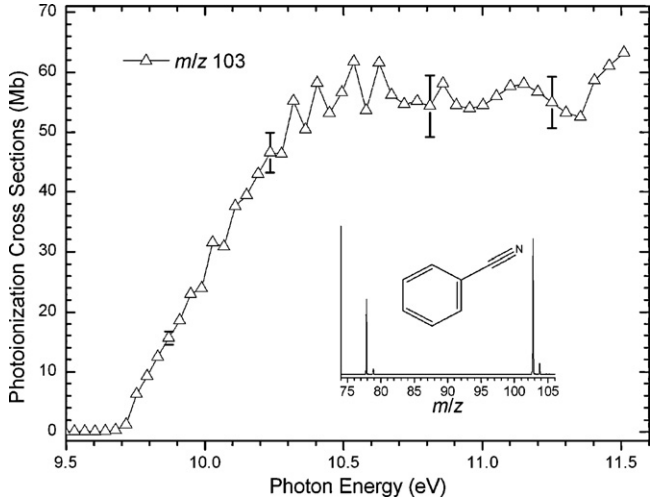

Fig. 23. Absolute photoionization cross-sections of benzonitrile. The error bars denote standard deviations of two replicates with separately prepared binary mixtures. The inserted figure displays the photoionization mass spectrum at the photon energy of 10.5 eV.

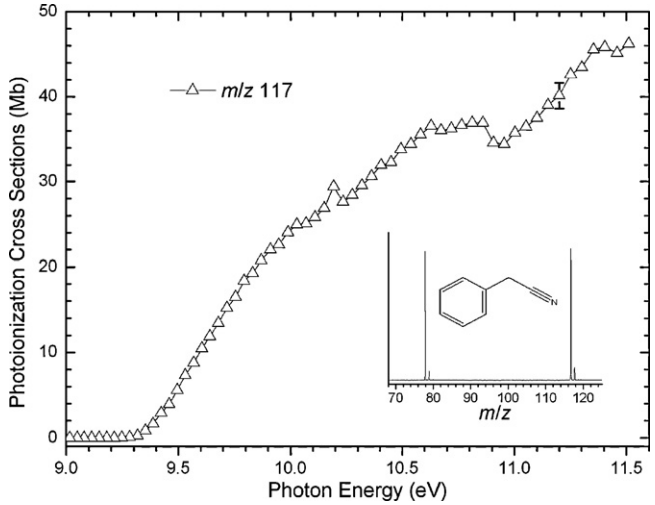

Fig. 24. Absolute photoionization cross-sections of benzeneacetonitrile. The error bars denote standard deviations of two replicates with separately prepared binary mixtures. The inserted figure displays the photoionization mass spectrum at the photon energy of 10.5 eV.

3.3. Diethylamine, dibutylamine and triethylamine

Figs. 7–9 display the absolute photoionization cross-sections of diethylamine, dibutylamine and triethylamine, respectively. Diethylamine is used as a corrosion inhibitor and in the production of rubber, resins, dyes and pharmaceuticals [34–38]. As shown in Fig. 7, IE (8.03 ± 0.05 eV) of $C_4H_{11}N$ is in good agreement with the literature value (8.01 ± 0.01 eV) measured by Watanabe et al. [21]. The AE of the major fragment $CH_3CH_2NHCH_2^+$ (m/z 58) via demethylation is 8.79 ± 0.05 eV. It is lower than the value (8.92 eV) reported by Lossing et al. [27] and much lower than the value (9.55 ± 0.05 eV) measured by Collin and Franskin [39], but both previous studies using EI method. The fragment $CH_3CHNHCH_2CH_3^+$ (m/z 72) via dehydrogenation of αC and $CH_3CH_2NH^+$ (m/z 44) by C–N bond cleavage are also observed in this work but with minor contribution to the total cross-sections.

Dibutylamine is also used as a corrosion inhibitor, in the manufacture of emulsifiers, and as a flotation agent [40]. In Fig. 8, the total cross-sections of dibutylamine are mainly attributed to the parent ion $C_8H_{19}N^+$ (m/z 129) and the major fragment $CH_3CH_2CH_2CH_2NHCH_2^+$ (m/z 86) by αC–βC bond cleavage. IE of dibutylamine is 7.70 ± 0.05 eV, which is in good agreement with the literature value (7.69 ± 0.03 eV) measured by Watanabe et al. [21]. Minor fragment $CH_3CH_2CH_2CHNHCH_2CH_2CH_2CH_3^+$ (m/z 128) via dehydrogenation of αC and $CH_3NHCH_2^+$ (m/z 44) via elimination of propylene (C_3H_6) from $CH_3CH_2CH_2CH_2NHCH_2^+$ and H-transfer are also observed in this work.

Triethylamine is mainly used in the production of quaternary ammonium compounds for textile auxiliaries and quaternary ammonium salts of dyes [41], which is also employed as an intermediate for manufacturing medicines, pesticides and other chemicals [42,43]. The photoionization and photodissociation cross-sections of triethylamine are shown in Fig. 9. The parent ion $C_6H_{15}N^+$ (m/z 101) rises up to a plateau from its molecular IE (7.45 ± 0.05 eV), which is close to the literature value (7.50 ± 0.02 eV) measured by Watanabe et al. [21]. The major fragment $(CH_3CH_2)_2NCH_2^+$ (m/z 86) via demethylation is observed at the AE 8.44 ± 0.05 eV, which is much lower than the value (11.48 eV) by EI method [44]. The minor fragment $(CH_3CH_2)_2NCHCH_3^+$ (m/z 100) via dehydrogenation of αC of is also observed in this work. The uncertainty for photoionization cross-section measurement of diethylamine, dibutylamine and triethylamine is less than ±25%.

3.4. Aniline, benzylamine, n-methylaniline and cyclohexanamine

Aniline is a precursor to many industrial chemicals, the main usage of which is in the manufacture of precursors to polyurethane [45]. The photoionization cross-section of aniline is shown in Fig. 10. Only the parent ion is observed in this work from its IE at 7.69 ± 0.05 eV, which agrees with the reference data (7.720 ± 0.002 eV by Hager et al. [46], 7.70 ± 0.1 eV by Potapov and Iskakov [47] and 7.67 ± 0.03 eV by Akopyan and Vilesov [48]).

Benzylamine is used as a masked source of ammonia [49]. As shown in Fig. 11, the cross-sections rise up to a plateau from the ionization threshold (8.58 ± 0.05 eV), which agrees with the reference data (8.64 ± 0.05 eV) reported by Vilesov and Terenin [50]. The major fragment observed in this work is $C_6H_5CHNH_2^+$ (m/z 106) via dehydrogenation of α-C with the AE at 9.14 ± 0.05 eV, which is close to the literature value (9.21 ± 0.07 eV) measured by Akopyan et al. [51]. The minor fragment $CH_2NH_2^+$ (m/z 30) by C–C single bond cleavage and $C_6H_6^+$ (m/z 78) via H-transfer from NH_2 group are also observed, but only makes little contribution to the total cross-sections.

As an isomer of toluidine, *n*-methylaniline is mainly used in the production of dyes [52]. Fig. 12 shows the photoionization and pho-

todissociation cross-sections of *n*-methylaniline. The IE of C_7H_9N is 7.34 ± 0.05 eV, which is in good agreement with the literature value 7.34 ± 0.02 eV reported by Vilesov and Terenin [50] and in accord with the data 7.30 ± 0.05 eV measured by Akopyan and Vilesov [48]. The major fragment is $C_6H_5NHCH_2^+$ (m/z 106) via dehydrogenation from methy group with the AE at ~10.5 eV. Minor fragment $C_6H_6^+$ (m/z 78) by C–N bond cleavage and H-transfer from CH_3 group is also observed in this work. In the process of analyzing both toluidine and *n*-methylaniline samples, the interference of peak of $C_6H_6^+$ (m/z 78) is considered for the same mass charge ratio with the standard species. Pure sample was tested in the same photon energy range and the interference of $C_6H_6^+$ (m/z 78) was deduced from the signal of benzene (the standard species).

Cyclohexylamine is used as an intermediate in synthesis of some herbicides, antioxidants, accelerators for vulcanization, pharmaceuticals, corrosion inhibitors, some sweeteners, etc. [53–56]. The photoionization and photodissociation cross-sections of cyclohexanamine are displayed in Fig. 13. The IE of $C_6H_{13}N$ is 8.40 ± 0.1 eV, which agrees with the literature value (8.4 ± 0.1 eV) by the photoelectron spectroscopy (PE) method [33]. The main fragments may be $CH_2CH_2CH_2CHNH^+$ (m/z 70) and $CH_2CH_2CHNH^+$ (m/z 56) via a ring-open and H-transfer process with elimination of an ethyl radical and a propyl radical, with appearance energies at 9.38 and 9.49 ± 0.05 eV, respectively. The uncertainties for photoionization cross-section measurements of aniline, benzylamine, *n*-methylaniline and cyclohexanamine are all less than ±25%.

3.5. Nitromethane, nitroethane, n-nitropropane and nitrobenzene

The principal use of nitromethane is as a stabilizer for chlorinated solvents, which is used in dry cleaning, semiconductor and degreasing [57]. It is also used most effectively as a solvent or dissolving agent for acrylate monomers, such as cyanoacrylates [58]. As shown in Fig. 14, only the parent ion $CH_3NO_2^+$ (m/z 61) is observed in this work with its molecular IE at 11.05 ± 0.05 eV, which is in good agreement with the literature value (11.1 ± 0.05 eV by Lifshitz et al. [59] and 11.08 ± 0.03 eV by Watanabe et al. [21]).

Nitroethane is used as a fuel additive and a precursor to explosives [60]. It is also a useful solvent for polymers such as polystyrene and is particularly useful for dissolving cyanoacrylate adhesives [61]. Fig. 15 displays the photodissociation cross-section of nitroethane. The total cross-sections of nitroethane are almost attributed to the fragment $C_2H_5^+$ (m/z 29) via elimination of NO_2 group with the AE at 10.81 ± 0.05 eV, which is slightly lower than the value (11.0 eV) by EI method [62].

N-Nitropropane has wide applications in organic synthesis, rocket fuel and resin coating [63,64]. It is also used as a good solvent [65]. The photoionization cross-section of *n*-nitropropane is shown in Fig. 16. The fragment $C_3H_7^+$ (m/z 43) via elimination of NO_2 group makes major contribution to the total cross-sections with the AE at 10.67 ± 0.05 eV, which is close to the value (10.6 eV) by EI method [62].

Approximately 95% of nitrobenzene is consumed in the production of aniline [66]. In Fig. 17, the total cross-sections of nitrobenzene are mainly attributed to the parent ion $C_6H_5NO_2^+$ (m/z 123) with its IE at 9.79 ± 0.05 eV, which is slightly lower than the literature values, i.e., 9.87 ± 0.05 eV by Matyuk et al. [67]; 9.85 ± 0.03 eV by Kotov and Potapov [68] and 9.92 eV by Watanabe et al. [21]. The fragments $C_6H_5O^+$ (m/z 93), $C_6H_5^+$ (m/z 77), NO^+ (m/z 30) and cyclopentadienyl radical cation ion ($C_5H_5^+$, m/z 65) are observed in this work, but make little contribution to the total cross-sections. The fragment $C_6H_5^+$ is formed directly via C–N bond cleavage, while the fragment $C_6H_5O^+$ and NO^+ are produced accompanied with an O-transfer process. The fragment $C_5H_5^+$ may be formed via some complicated ring-open and ring-close steps. The AE of $C_6H_5O^+$ (m/z 93) is 10.86 ± 0.1 eV, which agrees with the literature value (10.95 ± 0.05 eV) by Matyuk et al. [67] For fragment $C_6H_5^+$ (m/z 77), the AE in this work is 9.32 ± 0.15 eV, which is lower than the literature value (9.46 ± 0.05 eV) by Matyuk et al. [67]. The AE (10.9 ± 0.1 eV) of NO^+ (m/z 30) in this work is in good agreement with the value 10.89 ± 0.04 eV by the photoion-photoelectron coincidence spectroscopy (PIPECO) method [69]. The uncertainties for photoionization cross-section measurement of nitromethane, nitroethane, *n*-nitropropane and nitrobenzen are all less than ±25%.

3.6. Pyrrole, pyridine, pyrrolidine and morpholine

Pyrrole is mainly used as a standard species in chromatogram analysis [70]. Pyridine is an important solvent and reagent in organic synthesis [71]. For pyrrole (Fig. 18) and pyridine (Fig. 19), only the parent ions $C_4H_5N^+$ (m/z 67) and $C_5H_5N^+$ (m/z 79) are observed, respectively. The IE of pyrrole is 8.21 ± 0.05 eV, which agrees with the literature value by PI method (8.207 ± 0.003 eV by Cooper et al. [72]; 8.208 ± 0.005 eV by Williamson et al. [73]; 8.20 ± 0.01 eV by Potapov and Yuzhakova [74] and 8.20 ± 0.01 eV by Watanabe et al. [21]). The IE of pyridine is 9.24 ± 0.05 eV, which agrees with the reference value by PI method as well (9.25 eV by Eland et al. [75]; 9.30 ± 0.01 eV by Potapov and Yuzhakova [74]; 9.20 ± 0.05 eV by Akopyan and Vilesov [48]; 9.23 ± 0.03 eV by Watanabe [76]).

Pyrrolidine is used for producing pharmaceuticals, pesticides and antiseptics [77]. Morpholine is a good solvent for resin, olefin, shell-lac and also used as a reagent for analysis [78,79]. Figs. 20 and 21 display the photoionization and photodissociation cross-sections of pyrrolidine and morpholine, respectively. The total cross-sections of pyrrolidine are mainly attributed to the parent ion $C_4H_9N^+$ (m/z 71) and fragment ions $C_4H_8N^+$ (m/z 70) via dehydrogenation of αC and $CH_2CHNH_2^+$ (m/z 43) via elimination of C_2H_4 and H-transfer. The IE of pyrrolidine in this work is 8.27 ± 0.05 eV, lower than the literature value (8.41 eV) by PE method [80]. The AEs of fragment ions $C_4H_8N^+$ (m/z 70) and $CH_2CHNH_2^+$ (m/z 43) are 9.15 ± 0.05 eV and 9.92 ± 0.05 eV, respectively, lower than the literature value by EI method (11.0 ± 0.2 eV and 12.3 ± 0.2 eV by Gallegos and Kiser [81]). The total cross-sections of morpholine are mainly attributed to the parent ion $C_4H_9NO^+$ (m/z 87) and fragment ions $C_4H_8NO^+$ (m/z 86) via dehydrogenation of αC and $NHCHCHO^+$ (m/z 57) via elimination of an ethyl radical. The IE of morpholine is 8.24 ± 0.05 eV, much lower than the value by PE method (8.88 ± 0.05 eV by Domelsmith and Houk [82] and 8.91 ± 0.03 eV by Colonna et al. [83]). The AEs of fragment ions $C_4H_8NO^+$ (m/z 86) and $NHCHCHO^+$ (m/z 57) are 8.92 ± 0.1 eV and 9.54 ± 0.05 eV, respectively. The uncertainties for photoionization cross-section measurement of pyrrole, pyridine, pyrrolidine and morpholine are all less than ±25%.

3.7. N,N-Dimethylethanolamine

N,*N*-Dimethylethanolamine, also known as DMAE, is used in the synthesis of dyestuffs, textile auxiliaries, pharmaceuticals, emulsifiers and corrosion inhibitors [84–87]. The absolute photoionization and photodissociation cross-sections of *N*,*N*-dimethylethanolamine are shown in Fig. 22. The parent ion $C_4H_{11}NO^+$ (m/z 89) rises slowly up to a plateau of about 3 Mb from its IE at 8.03 ± 0.1 eV, which is much lower than the literature value (8.80 eV by Ohno et al. [88]; 8.82 eV by Wieczorek et al. [89] and 8.85 ± 0.04 eV by Leavell et al. [90]) by PE method. Only the fragment $(CH_3)_2NCH_2^+$ (m/z 58) by C–C bond cleavage is observed in this work with the AE at 8.55 ± 0.05 eV, which is a little lower than the value (8.68 eV) by EI method [27]. The uncertainty for photoionization cross-section measurement of *N*,*N*-dimethylethanolamine is less than ±25%.

3.8. Benzonitrile and benzeneacetonitrile

Benzonitrile is a useful solvent and a versatile precursor for many derivatives [91]. Benzeneacetonitrile is used for the production of pharmaceuticals and intermediates of pesticides [92]. As shown in Figs. 23 and 24, only parent ions of benzonitrile and benzeneacetonitrile are observed in this work. The IE of benzonitrile is 9.67 ± 0.05 eV, which agrees with the literature value (9.71 ± 0.01 eV) by Watanabe et al. [21]. The IE of benzeneacetonitrile is 9.32 ± 0.05 eV, which is in good agreement with the value (9.32 ± 0.05 eV) by EI method [93]. Considering the relatively large fluctuation of signals in the higher photon energy range for the repeated measurements, the uncertainties for photoionization cross-section measurement of benzonitrile and benzeneacetonitrile are both estimated in the region of ±25–35%.

4. Conclusion

Experimental determination of absolute photoionization cross-sections for 24 nitrogenous compounds was performed over the energy range of 7.2–11.5 eV with tunable synchrotron VUV photoionization and molecular-beam mass spectrometry. All of these data are useful for quantitative analysis of these compounds involving photoionization process. In special, it is important for calculating the concentrations of some nitric combustion intermediates, which are essential for kinetic modeling study in relevant combustion chemistry. The binary-liquid-mixture method used in this experiment has been proved to be feasible and reliable for species that can form solution. But the method is limited when it is extended to determine the photoionization cross-sections of solid compound with higher boiling point and lower stability.

Supporting information

Tabulated photoionization cross-sections for the species measured in the present work are available in the online version of this article.

Acknowledgement

This work was supported by Chinese Academy of Sciences and Natural Science Foundation of China (50925623).

Appendix A. Supplementary data

Supplementary data associated with this article can be found, in the online version, at doi:10.1016/j.ijms.2011.01.024.

References

[1] M.L. Gorbaty, S.R. Kelemen, Fuel Process. Technol. 71 (2001) 71.
[2] G. Di Nola, W. de Jong, H. Spliethoff, Fuel Process. Technol. 91 (2010) 103.
[3] J. Giuntoli, W. de Jong, A.H.M. Verkooijen, P. Piotrowska, M. Zevenhoven, M. Hupa, Energy Fuels 24 (2010) 5309.
[4] Z. Tian, Y. Li, T. Zhang, A. Zhu, Z. Cui, F. Qi, Combust. Flame 151 (2007) 347.
[5] Z. Tian, Y. Li, T. Zhang, A. Zhu, F. Qi, J. Phys. Chem. A 112 (2008) 13549.
[6] A. Lucassen, P. Oßwald, U. Struckmeier, K. Kohse-Höinghaus, T. Kasper, N. Hansen, T.A. Cool, P.R. Westmoreland, Proc. Combust. Inst. 32 (2009) 1269.
[7] Z. Tian, L. Zhang, Y. Li, T. Yuan, F. Qi, Proc. Combust. Inst. 32 (2009) 311.
[8] Y. Li, F. Qi, Acc. Chem. Res. 43 (2010) 68.
[9] T. Adam, R. Zimmermann, Anal. Bioanal. Chem. 389 (2007) 1941.
[10] D.A. Shaw, D.M.P. Holland, J. Phys. B: At. Mol. Opt. Phys. 41 (2008) 10.
[11] T. Masuoka, A. Kobayashi, Chem. Phys. 302 (2004) 31.
[12] T.J. Xia, T.S. Chien, C.Y.R. Wu, D.L. Judge, J. Quant. Spectrosc. Radiat. Transf. 45 (1991) 77.
[13] M. Suto, L.C. Lee, J. Chem. Phys. 78 (1983) 4515.
[14] I. Cacelli, V. Carravetta, J. Phys. B: At. Mol. Opt. Phys. 29 (1996) 3363.
[15] G.M. Seabra, I.G. Kaplan, V.G. Zakraewski, J.V. Ortiz, J. Chem. Phys. 121 (2004) 4143.
[16] E.M. Nascimento, E.M.S. Ribeiro, L.M. Brescansin, M.T. Lee, L.E. Machado, J. Phys. B: At. Mol. Opt. Phys. 36 (2003) 3621.
[17] Z. Zhou, M. Xie, Z. Wang, F. Qi, Rapid Commun. Mass Spectrom. 23 (2009) 3994.
[18] Z. Zhou, L. Zhang, M. Xie, Z. Wang, D. Chen, F. Qi, Rapid Commun. Mass Spectrom. 24 (2010) 1335.
[19] M. Xie, Z. Zhou, Z. Wang, D. Chen, F. Qi, Int. J. Mass Spectrom. 293 (2010) 28.
[20] E.E. Rennie, C.A.F. Johnson, J.E. Parker, D.M.P. Holland, D.A. Shaw, M.A. Hayes, Chem. Phys. 229 (1998) 107.
[21] K. Watanabe, T. Nakayama, J.R. Mottl, J. Quant. Spectrosc. Radiat. Transf. 2 (1962) 369.
[22] W.A. Chupka, J. Chem. Phys. 30 (1959) 191.
[23] S. Gabriel, A.-S. Duwez, R. Jérôme, C. Jérôme, Langmuir 23 (2006) 159.
[24] J. Schonherr, Pest Manage. Sci. 58 (2002) 343.
[25] C. Brunellil, Y. Zha, M.H. Brown, P. Sandra, J. Sep. Sci. 31 (2008) 1299.
[26] B.H. Solka, M.E. Russell, J. Chem. Phys. 78 (1974) 1268.
[27] F.P. Lossing, Y.T. Lam, A. Maccoll, Can. J. Chem. 59 (1981) 2228.
[28] I. Onyido, J.E. Omakor, G.W. vanLoon, E. Buncel, Arkivoc 2 (2001) U114.
[29] M. Medenica, D. Ivanovic, M. Magkovic, B. Jancic, A. Malenovic, J. Pharm. Biomed. Anal. 44 (2007) 1087.
[30] M. Starek, J. Krzek, M. Tarsa, M. Zylewski, Chromatographia 69 (2009) 351.
[31] C.H. Baek, J.Y. Kong, S.H. Hyun, Y.J. Lim, W.S. Kim, Polymer-Korea 29 (2005) 433.
[32] J.L. Holmes, F.P. Lossing, A. Maccoll, J. Am. Chem. Soc. 110 (1988) 7339.
[33] D.H. Aue, H.M. Webb, M.T. Bowers, J. Am. Chem. Soc. 98 (1976) 311.
[34] R.T. Vashi, S.A. Desai, P.S. Desai, Asian J. Chem. 20 (2008) 4553.
[35] W. Huang, Y. Ikeda, A. Oku, Polymer 43 (2002) 7295.
[36] M.S. Filigenzi, B. Puschner, L.S. Aston, R.H. Poppenga, J. Agric. Food Chem. 56 (2008) 7593.
[37] J.R. de la Fuente, C. Jullian, C. Saitz, V. Neira, O. Poblete, E. Sobarzo-Sanchez, J. Org. Chem. 70 (2005) 8712.
[38] D.B. Pathare, A.S. Jadhav, M.S. Shingare, J. Pharm. Biomed. Anal. 41 (2006) 1152.
[39] J.E. Collin, M.J. Franskin, Bull. Soc. R. Sci. Liège 35 (1966) 285.
[40] J.M. Bastidas, J. de Damborenea, A.J. Vazquez, J. Appl. Electrochem. 27 (1997) 345.
[41] Y. Yang, H. Imaoka, K. Yamashita, N. Kamogawa, H. Watanabe, M. Miyazaki, Y. Oki, Jpn. J. Appl. Phys. 49 (2010) 3.
[42] H.S. Wu, C.W. Lo, J. Comb. Chem. 8 (2006) 848.
[43] E.R. Kenawy, F.I. Abdel-Hay, A. Abou El-Magd, Y. Mahmoud, React. Funct. Polym. 66 (2006) 419.
[44] V.F. Plotnikov, G.M. Bogolyubov, I.A. Maretina, A.A. Petrov, Zh. Org. Khim. 5 (1969) 1137.
[45] E.C. Buruiana, M. Olaru, M. Strat, G. Strat, B.C. Simionescu, Polym. Int. 54 (2005) 1296.
[46] J. Hager, M. Smith, S. Wallace, J. Chem. Phys. 83 (1985) 4820.
[47] V.K. Potapov, L.I. Iskakov, High Energy Chem. 5 (1971) 237.
[48] M.E. Akopyan, F.I. Vilesov, Dokl. Akad. Nauk SSSR 158 (1964) 1386.
[49] V.J. Gatto, S.R. Miller, G.W. Gokel, Org. Synth. 68 (1990) 227.
[50] F.I. Vilesov, A.N. Terenin, Dokl. Akad. Nauk SSSR 115 (1957) 744.
[51] M.E. Akopyan, F.I. Vilesov, A.N. Terenin, Dokl. Akad. Nauk SSSR 140 (1961) 1037.
[52] J.J. Yin, G. Ye, X.G. Wang, Langmuir 26 (2010) 6755.
[53] N.J. Novick, M. Alexander, Appl. Environ. Microbiol. 49 (1985) 737.
[54] H. Nayyar, S. Chander, J. Agron. Crop Sci. 190 (2004) 355.
[55] M.H.S. Gradwell, W.J. McGill, J. Appl. Polym. Sci. 61 (1996) 1515.
[56] D.Q. Zhang, Z.X. An, Q.Y. Pan, L.X. Gao, G.D. Zhou, Corros. Sci. 48 (2006) 1437.
[57] K. Mori, Y. Nakamura, M. Kaneko, T. Kan, H. Nakamura, Jpn. J. Toxicol. Environ. Health 39 (1993) 317.
[58] A. Balent, Am. J. Ophthalmol. 82 (1976) 501.
[59] C. Lifshitz, M. Rejwan, I. Levin, T. Reres, Int. J. Mass Spectrom. Ion Process. 84 (1988) 271.
[60] S. Courtecuisse, F. Cansell, D. Fabre, J.P. Petitet, J. Chem. Phys. 108 (1998) 7350.
[61] H.C. de Sousa, L.P.N. Rebelo, J. Chem. Thermodynam. 32 (2000) 355.
[62] S. Tsuda, W.H. Hamill, Adv. Mass Spectrom. 3 (1966) 249.
[63] G.Z. Liu, Y.J. Han, L. Wang, X.W. Zhang, Z.T. Mi, Energy Fuels 23 (2009) 356.
[64] R. Harrison, G. Letz, G. Pasternak, P. Blanc, Ann. Intern. Med. 107 (1987) 466.
[65] G. Wu, J.C. Chabot, J.J. Caron, M. Heitz, Water Air Soil Pollut. 101 (1998) 69.
[66] G. Booth, Nitro compounds, aromatic, in: Ullmann's Encyclopedia of Industrial Chemistry, John Wiley & Sons, New York, 2000.
[67] V.M. Matyuk, V.K. Potapov, A.L. Prokhoda, Russ. J. Phys. Chem. 53 (1979) 538.
[68] B.V. Kotov, V.K. Potapov, Khim. Vys. Energy 6 (1972) 375.
[69] T. Nishimura, P.R. Das, G.G. Meisels, J. Chem. Phys. 84 (1986) 6190.
[70] H. Bagheri, A. Mohammadi, A. Salemi, Anal. Chim. Acta 513 (2004) 445.
[71] L. Christensen, R. Fitzpatrick, B. Gildea, K.H. Petersen, H.F. Hansen, T. Koch, M. Egholm, O. Buchardt, P.E. Nielsen, J. Coull, R.H. Berg, J. Pept. Sci. 1 (1995) 175.
[72] C.D. Cooper, A.D. Williamson, J.C. Miller, R.N. Compton, J. Chem. Phys. 73 (1980) 1527.
[73] A.D. Williamson, R.N. Compton, J.H.D. Eland, J. Chem. Phys. 70 (1979) 590.
[74] V.K. Potapov, O.A. Yuzhakova, Dokl. Akad. Nauk SSSR 192 (1970) 131.
[75] J.H.D. Eland, J. Berkowitz, H. Schulte, R. Frey, Int. J. Mass Spectrom. Ion Phys. 28 (1978) 297.
[76] K. Watanabe, J. Chem. Phys. 26 (1957) 542.
[77] A.J. Smit, J. Appl. Phycol. 16 (2004) 245.
[78] E. Chargaff, C. Levine, C. Green, J. Biol. Chem. 175 (1948) 67.
[79] W. Schwack, S. Nyanzi, Fres. J. Anal. Chem. 345 (1993) 705.
[80] M.I. Al-Joboury, D.W. Turner, J. Chem. Soc. (1964) 4434.
[81] E.J. Gallegos, R.W. Kiser, J. Phys. Chem. 66 (1962) 136.
[82] L.N. Domelsmith, K.N. Houk, Tetrahedron Lett. 23 (1977) 1981.

[83] F.P. Colonna, G. Distefano, S. Pignataro, G. Pitacco, E. Valentin, J. Chem. Soc., Faraday Trans. 71 (1975) 1572.
[84] T. Uchida, S. Yamashita, Biochim. Biophys. Acta 1043 (1990) 281.
[85] C. Wang, F.N. Jones, J. Appl. Polym. Sci. 78 (2000) 1698.
[86] V.R. Shanbhag, A.M. Crider, R. Gokhale, A. Harpalani, R.M. Dick, J. Pharm. Sci. 81 (1992) 149.
[87] C.R. Brundle, M. Grunze, U. Mäder, N. Blank, Surf. Interf. Anal. 24 (1996) 549.
[88] K. Ohno, K. Imai, Y. Harada, J. Am. Chem. Soc. 107 (1985) 8078.
[89] J.S. Wieczorek, T. Koenig, T. Balle, J. Electron Spectrosc. Relat. Phenom. 6 (1975) 215.
[90] S. Leavell, J. Steichen, J.L. Franklin, J. Chem. Phys. 59 (1973) 4343.
[91] R.A. Nyquist, Appl. Spectrosc. 44 (1990) 1405.
[92] A.K. Amirjahed, M.I. Blake, J. Pharm. Sci. 63 (1974) 696.
[93] E.T. Selim, M.A. Rabbih, M.A. Fahmey, Org. Mass Spectrom. 22 (1987) 381.